DOI: 10.5281/zenodo.6967186

Project	GUTTA
Work Package number	3
Work Package title	Strategic potential for a greener and more integrated CB maritime mobility
Deliverable number	D 3.2.2
Deliverable title	Harmonized and queriable database of vessel propulsion and performance data
Deliverable Responsible Partner	UniZd
Deliverable Lead authors	J. Orović (UniZd), Z. Pavin (UniZd), G. Mannarini (CMCC), L.Carelli (CMCC)
Deliverable Contributors	M. Barić (UniZd), R. Jelić (UniZd), V. Knežević (UniZd)
Deliverable due date	2019-12-31
Deliverable latest review date	2020-03-19

Table of Contents

Executive Summary

This document reports about a new database of propulsion and performance data of a specific RoPax vessel. The database originates from systematic runs of a nautical simulator operating at UniZd. Resulting data are fitted by a multi-dimensional model developed and implemented by CMCC. The functional dependence of both speed and engine power as functions of the meteo-marine variables are reconstructed.

List of abbreviations

In addition to the GUTTA Glossary (https://zenodo.org/record/3676344), following abbreviations are used in this deliverable report:

CPP: Controllable pitch propeller

kt: knot(s)

MCR: Maximum Continuous Rating of main engine(s)

nmi: nautical mile(s)

SI: International System of Units

SOG: Speed over Ground

STW: Speed Through Water

1. Introduction

The goal of GUTTA deliverable D.3.2.2 is to create a harmonized and queriable database of RoPax vessel propulsion and performance in presence of various meteo-marine conditions.

This task is split into the present deliverable, where just the vessel speed and power are considered and D. 4.1.1, where CO2 emission data will also be considered.

Two simulators were purchased by UniZd with partial funding from GUTTA project. Installation of the simulators was a quite demanding activity, in particular in order to achieve a joint operation between the bridge and the engine room simulator. Therefore, the data collection phase extended even beyond RP2 (the reporting period this deliverable refers to).

The report is organized into a description of the methodology (simulators and data processing), in Sect.2, and presentation of the results, in Sect.3. The conclusions are drawn in Sect.4

2. Methodology

The simulators are described in Section 2.1, the vessel type in Section 2.2., and the data collection protocol in Section 2.3.

2.1 Simulators

The UniZd marine simulator, shown in Figure 1, consists of:

A. a fully integrated command bridge,
B. a fully integrated engine control room,
C. modern cabinet with nautical simulators with a global alert, search and rescue system, ship to shore communication (GMDSS – Global maritime distress and safety system),
D. modern cabinet equipped with engine room simulators with diesel, steam turbine and diesel-electric propulsion systems and cargo handling simulators for crude oil carrier tankers and LNG tankers.

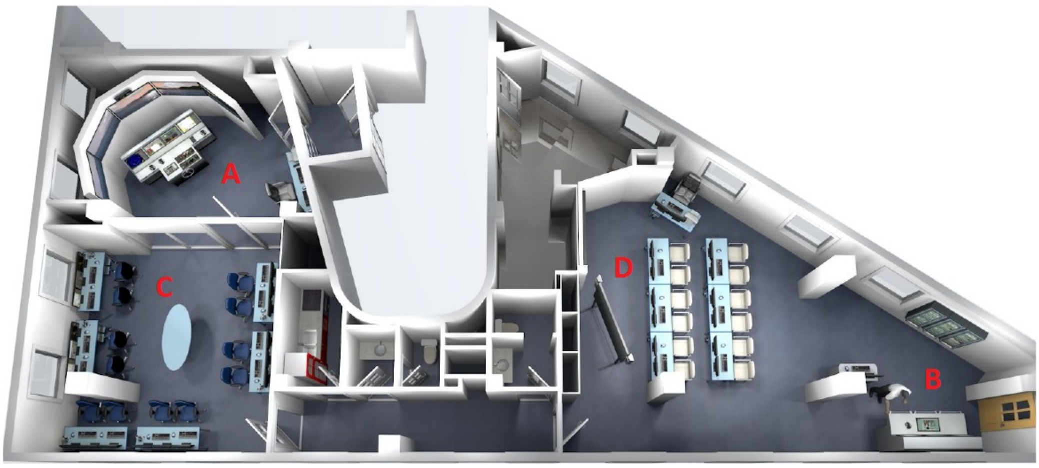

Figure 1 Layout of simulator rooms at UniZd. The letters correspond to the components described in the text.

The simulator complies with the STCW 2010 Convention that regulates simulator equipment to be used for training of seafarers[1]. The functionality of the simulator was verified by the CRS (Croatian Register of Shipping), a certified member organization of the IACS (International Association of Classification Societies). The company that developed the simulator software owns a valid certificate in compliance with both ISO 9001 and ISO 12207 standards.

1) The bridge simulator "Wärtsilä-Transas Marine NTPro 5000 Navigation Simulator"[2] consists of a "Full mission" command bridge simulator with a realistic console (Fig.2) and an additional classroom with ECDIS/Radar/GMDSS simulators on six student stations and an instructor console

Figure 2 NTPro 5000 Navigation Simulator - command bridge console

[1] http://www.imo.org/en/OurWork/HumanElement/TrainingCertification/Pages/STCW-Convention.aspx

[2] https://www.Wartsila.com/docs/default-source/product-files/optimise/simulation-and-training/navigational-simulators-brochure.pdf

The command bridge is equipped with a 150 degree-wide visualisation on five visualisation channels, two multifunctional radar monitors and one ECDIS Conning display, a GMDSS station and two overhead channels, control command telegraph for astern thruster, bow thruster and azimuth thrusters. Fifteen different vessel types can be simulated and fifteen different navigation areas can be used. Numerous dynamic parameters that affect the ship's hull during navigation can be varied.

2) The engine room simulator and cargo handling simulator "Wärtsilä ERS-LCHS 5000 TechSim"[3], consists of a classroom with one instructor console, six student stations and a realistic engine control room with a control console, local unit, main switchboard and a high voltage simulator (Fig.3.a,b).

a) b)

Figure 3 a) engine control room simulator; b) classroom with six student stations and instructor console.

All stations can simulate six different engine room and cargo handling models.

[3] https://www.Wärtsilä.com/marine/optimise/simulation-and-training/technological-simulators/ers-5000-engine-room-simulator

2.2 Vessel type

Only one vessel type could be funded through the GUTTA project. It is a RoPax Ferry with MAN Diesel 32/40 Twin Medium Speed Engine with controllable pitch propeller (CPP), whose technical specifications are provided in Fig. 4.

A simulated vessel type is a software add-on which is added and integrated into the already existing main ERS 5000 Techsim platform by Transas and can be simulated on any ERS classroom or engine control room station.

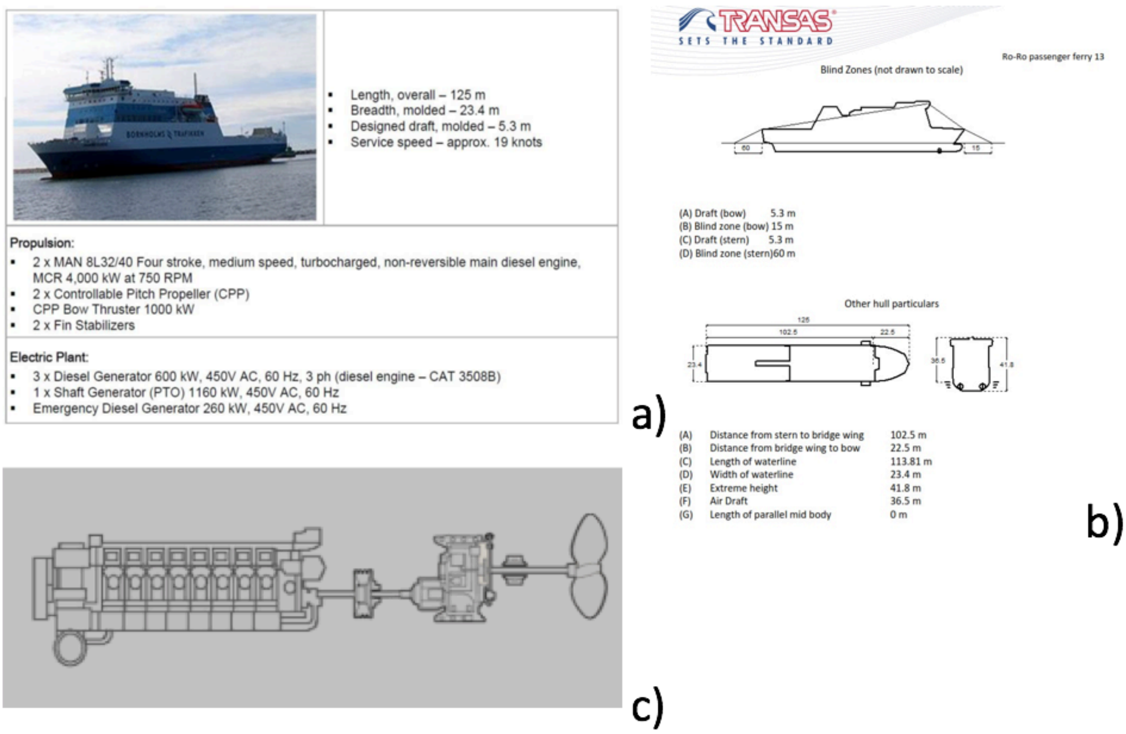

Figure 4 Technical specifications of the vessel type that can be simulated at UniZd. a) vessel principal particulars and propulsion parameters; b) hull and superstructure geometry; c) layout of main engine with clutch, reduction gear and propeller.

2.3. Data collection procedure and analysis protocol

The coupled operation mode of the engine room simulator and the bridge simulator is quite time-expensive. This is in view of delivering a higher level of accuracy in the resulting vessel response. For this first phase of the GUTTA project though, only the nautical simulator is used. The coupled operation mode will be utilized in the next project phase, in order to allow for more accurate engine room parameters to be collected and to enable direct simulation of CO_2 emissions.

The simulated vessel performance is based on observed navigational data which is not further disclosed nor documented by the manufacturer. Therefore, our approach for extracting the vessel response in presence of several different meteo-marine conditions was to:

- Generate realistic combinations of meteo-marine conditions;
- record the corresponding simulator response;
- analyse the results by fitting a regression model.

The environmental state is represented within the simulator by discretization of variables such as significant wave height (Hs), wave relative direction (Ψ), wind speed (U) and its direction relative to vessel (Ψ). The vessel behaviour is driven by the percentage of engine MCR (i.e., position of the telegraph lever). The diagnostic variables are: vessel speed through water (SWT), delivered engine power (P), and engine revolutions per minute (rpm).

For each combination of these variables, a T_{rec} time has to be spent in data acquisition. This is due to the fact that the simulated vessel requires a transient time for adjusting to the imposed simulated marine environment. All data recorded for each parameter during T_{rec} are then averaged in time. Given that T_{rec} is never lower than 20 minutes, if the data collection experiment is not carefully designed, the simulator time cost for all combinations of parameters can easily grow. Therefore, it is crucial to only perform simulations corresponding to the most relevant meteo-marine conditions. This not only means that e.g. waves and wind values are realistic, but also that they are chosen in a way to sample the vessel response where either its value or its gradient with respect to each variable of interest is most significant.

This is why an experimental approach was followed, collecting data by varying a single variable first. These 1D experiments provided in fact a guideline, for learning where the gradients in the vessel response are strongest. This insight was then used for devising an experiment with variations of multiple variables. The outcomes of this experimental protocol are documented in Sect.3.

3. Results

In all experiments, sea currents acting on the vessel were assumed to be null. This is done because SOG can be approximated to be given from the vector sum of STW and the sea current vector, using the method documented and used in Mannarini and Carelli (2019).

3.1 Realistic wind wave parametrization

A first needed input for the simulator was a realistic combination of wind and wave magnitudes, to drive the simulated vessel behaviour.

Farkas (2016) uses satellite data from the World Waves Atlas (Barstow 2003) referred to a location in the middle part of the Adriatic Sea (near Palagruža island). The author states that 10m height wind and significant wave height are used in the analysis. Limitations of this approach are that:

i) The data are quite scattered along the fitted regression line (even by a factor of 2 in some cases)

ii) They refer to a specific location where the prevailing winds are along the axis of the Adriatic (i.e. from either NW or SE) but also from NE, for which direction sea waves are likely fetch-limited.

In agreement with the dimensional argument by in Seck-Hong (1977), the fitted regression formula is quadratic in *U*:

$$H_s = a \cdot U^2 + b \cdot U \quad \text{(Eq.1)}$$

This relation can be inverted as:

$$U = \frac{-b + \sqrt{b^2 + 4aH_s}}{2a} \quad \text{(Eq.2)}$$

where the fit coefficients by Farkas (who displays U in m/s) are:

a= 0.0127 s^2/m

b= 0.0055 s

A sample evaluation of Farkas results is displayed in Figure 5, where also perturbations of the fit formula are added, to represent the scatter of Farkas' original data.

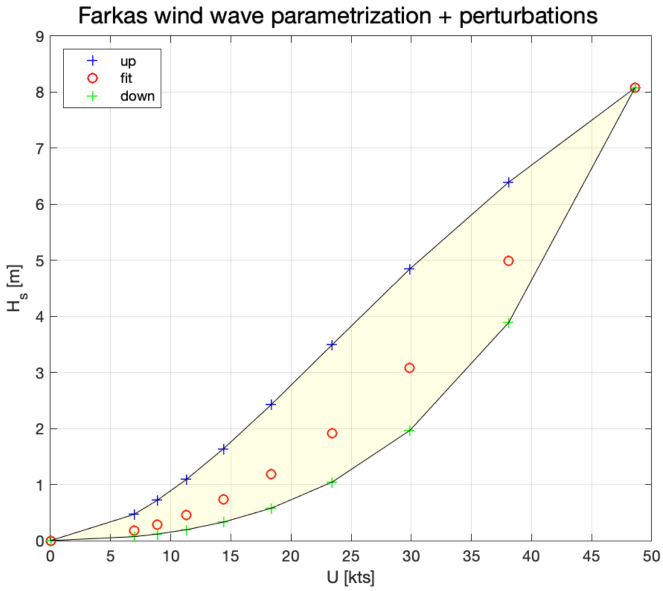

Figure 5 H from Farkas method. The "down" and "up" series have been rescaled by a U-dependent factor, in order to mime the variability in the data points displayed in Farkas 2016 (Figure 6)

3.2 Sensitivity study to wind-wave parametrization

Here the goal was to check how speed loss in waves changes depending on the actual parametrization of wind-waves depending on wind magnitude *U*.

For the same *U* value there are now 3 different *Hs* series "down", "fit", "and "up". They correspond to Farkas fit formula and its lower and upper perturbations as in Figure 5 of this document. The input parameters are shown in Table 1 and the results of the simulations are displayed in Figure 6. There also is a curve corresponding to the speed-loss curve computed by VISIR-1 (Mannarini et al, 2016) for a vessel with same size and engine parameters. In GUTTA project, a new model version VISIR-2 is being developed by CMCC and it will use the results documented in this report for the RoPax speed loss in waves and wind.

Table 1 Farkas DOWN, FIT and UP methods input parameters

Farkas DOWN		Farkas FIT		Farkas UP	
wind magnitude [kts]	sign. wave height (down) [m]	wind magnitude [kts]	sign. wave height (fit) [m]	wind magnitude [kts]	sign. wave height (up) [m]
0	0	0	0	0	0
6,9	0,1	6,9	0,2	6,9	0,5
8,9	0,1	8,9	0,3	8,9	0,7
11,3	0,2	11,3	0,5	11,3	1,1
14,4	0,3	14,4	0,7	14,4	1,6
18,4	0,6	18,4	1,2	18,4	2,4
23,4	1	23,4	1,9	23,4	3,5
29,9	2	29,9	3,1	29,9	4,8
38,1	3,9	38,1	5,0	38,1	6,4
48,6	8,1	48,6	8,1	48,6	8,1

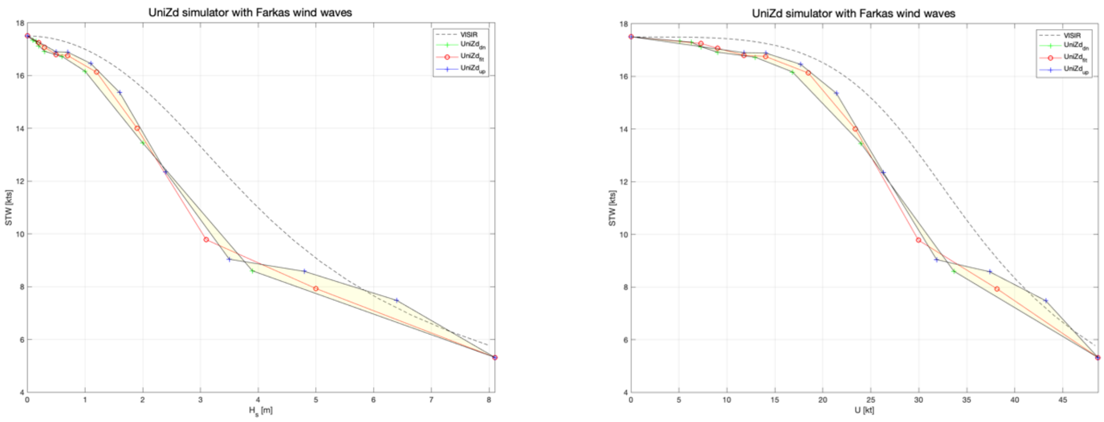

Figure 6 Markers with lines: Comparison of VISIR-1 speed loss function (black) to UniZd simulator results (magenta; "fit" series only). Left panel: dependence on significant wave height Hs; Right panel: dependence on wind magnitude U (computed through Eq.2). Note that VISIR presently only includes the effect of waves and neglects wind

The results allow to draw the following conclusions:

- the dependency of STW on actual wind-wave is relatively weak;
- there are three distinct speed loss regions:
  - Hs < 1 m | U < 17 kt (minor speed loss)
  - 1 m < Hs < 3.2m | 9 kt < U < 31 kt (steep increase of speed loss)
  - Hs > 3.2m | U > 31 kt (moderate additional speed loss)

- the agreement with VISIR-1 at large Hs should be considered accidental, as there are several guessed parameters in the VISIR-1 speed loss function.

3.3 Wind-waves vs. Swell

In order to assess the impact of the aerodynamic drag on the added resistance of the superstructure, the speed loss curve is then simulated using waves but switching wind off. We call this pseudo-swell, to contrast it with the simulator built-in swell that we want to compare to. The input parameters for the corresponding simulations are shown in Table 2.

Table 2 Wind-Wave and Swell variation input parameters. During the period of the simulation when the parameters shown in red were active the ship had to be manually controlled as it would turn off course with such low STW when on autopilot

MCR=90%, Wind=0kts	MCR=90%, Wind=0kts (with simulator built-in function SWELL)	Wind=26,1kts, Wave height=2,4m, MCR=90%	Wind=33,5kts, Wave height=3,9m, MCR=90%	Wind speed=26,1kts, Wave height=2,4m, Ψ=0°	Wind speed=0kts, Wave height=0m, Ψ=0°
Swell height (m)	Swell height (m)	Wave and wind direction	Wave and wind direction	MCR (%)	MCR (%)
0,0	0,0	0°	0°	90%	90%
0,2	0,2	18°	18°	85%	85%
0,3	0,3	36°	36°	80%	80%
0,5	0,5	54°	54°	70%	70%
0,7	0,7	72°	72°	60%	60%
1,2	1,2	90°	90°	50%	50%
1,9	1,9	108°	108°	40%	40%
3,1	3,1	126°	126°		
5,0	5,0	144°	144°		
8,1	8,1	162°	162°		
		180°	180°		

The results displayed in Figure 7 show that:

- the impact of the aerodynamic drag is small: it leads to additional speed loss always smaller than 0.5 kt;
- the simulator built-in swell leads to a fatter tail in the curve than the pseudo-swell, with about 2 kt less speed loss.

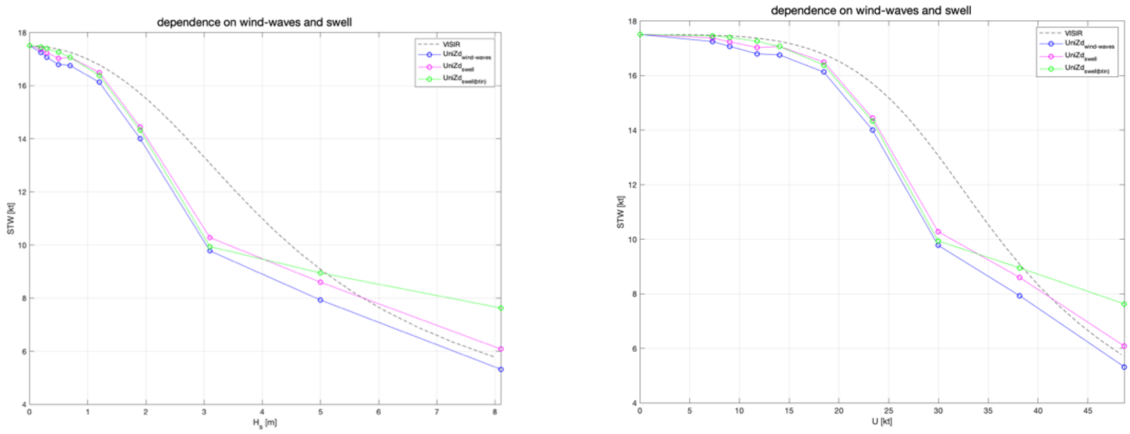

Figure 7 Speed loss curves for the Farkas fit formula (blue markers and lines), the case of no relative wind (magenta), and the simulator built-in representation of vessel-swell interaction (green). Left panel: dependence on significant wave height computed using Eq.2; Right panel: same results displayed with dependence on wind magnitude. Note that VISIR-1 only includes the effect of waves and neglects wind.

3.4 Multi-dimensional experiment

Having realized where the speed loss is and changes most, in a subsequent series of data collection experiments also:

- the relative direction of waves
- the percentage of MCR

were varied. For wind direction it was assumed that it is always collinear to wave direction. This is consistent with a prevailing wind-waves climate (i.e., negligible swell). In the Adriatic, where GUTTA project finally needs to use the outcome of the present simulations, this condition is usually met. Finally, 100 combinations of meteo-marine fields were chosen to drive the simulator data collection. In particular, the parameters used for multi-dimensional simulation set up were:

- Percentage Engine MCR: variable from 90% to 60% in steps of 10%
- Hs: [0, 2.5, 3, 3.5, 4] m
- Environmental load direction - Psi: [0, 50, 60, 70, 180] deg
- Wind: collinear with waves and intensity given by Farkas formula (Sect.3.1).

The main engines are controlled in combinator mode. In this mode the position of the telegraph lever corresponds to a certain combination of engine rpm and propeller pitch. Consequently, the MCR of the engine power at propeller shaft changes. Resulting STW, engine Power, and rpm were recorded and organized into a queriable database for enabling the subsequent analysis. It consisted in a multiple regression technique, implemented through a cascade of 1D least square fits.

Table 3 Parameter inputs for the STW, Power and RPM measurement simulations. This parameter input list was simulated with different MCR loads expressed here in percentages: 90, 80%, 70% and 60% loads. Red digits means that manual steering was needed.

Wind	Wave	Environmental load direction (true)
0	0	0
26,8551	2,5	0
29,4579	3	0
31,8514	3,5	0
34,0793	4	0
0	0	50
26,8551	2,5	50
29,4579	3	50
31,8514	3,5	50
34,0793	4	50
0	0	60
26,8551	2,5	60
29,4579	3	60
31,8514	3,5	60
34,0793	4	60
0	0	70
26,8551	2,5	70
29,4579	3	70
31,8514	3,5	70
34,0793	4	70
0	0	180

26,8551	2,5	180
29,4579	3	180
31,8514	3,5	180
34,0793	4	180

The relation of engine power with the position of the telegraph level (MCR) is shown in Fig.8 for various environmental loads (significant wave height values, Hs). A power-law dependence can be fitted at each Hs.

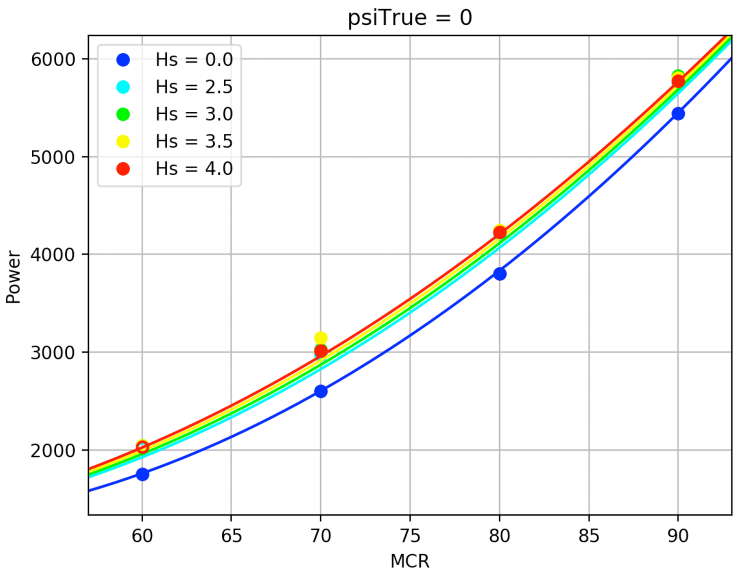

Figure 8 Engine power vs. %MCR for various sea state (labelled by significant wave height Hs) in case of head waves

The engine load diagram instead can be reconstructed by displaying the engine power at propeller shaft vs. engine speed (rpm), as done in Fig.9. The light and heavy running regimes correspond to parallel lines in this plane, the light running corresponding to the lower power.

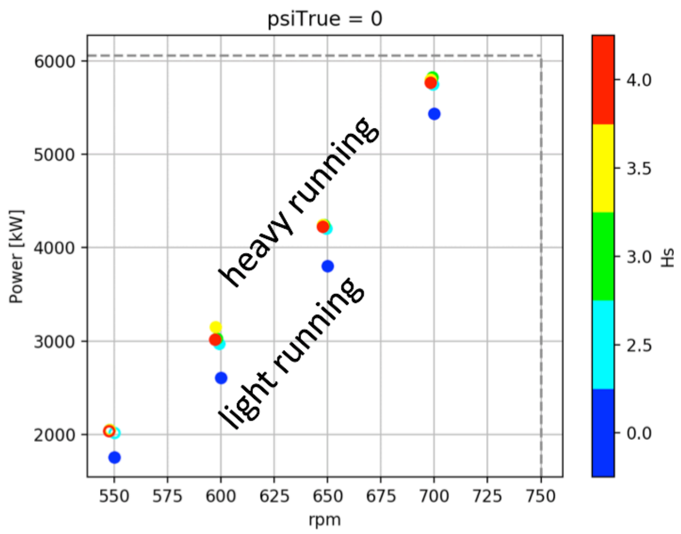

Figure 9 Engine load diagram for head waves (ψ=0). The grey dashed lines correspond to maximum engine power and engine velocity.

4. Conclusions

A database of vessel propulsion and performance data based on the response of a RoPax simulator was created and the underpinning functional dependence was identified.

The data collection was performed using the simulators installed at the University of Zadar and the data analysis was performed by CMCC using multi-dimensional regression. Both STW and engine power at propeller shaft were fitted as functions of significant wave height, relative wave direction, and engine telegraph lever.

The dataset and the regression technique here devised will be used also in deliverable D.4.1.1 for providing a parametrization of CO_2 emissions as a function of the meteo-marine conditions. This functional dependence is to be used in the VISIR-2 model, which is at the core of the eco-routes tool being developed within the GUTTA project.

Bibliography

S. Barstow et al., World Waves: Fusion of data from many sources in a user-friendly software package for timely calculation of wave statistics in global coastal waters, The Thirteenth International Offshore and Polar Engineering Conference. International Society of Offshore and Polar Engineers, 2003.

Farkas, A., Parunov, J. and Katalinić, M., 2016. Wave statistics for the middle Adriatic Sea. Pomorski zbornik, 52(1), pp.33-47.

G. Mannarini, N. Pinardi, G. Coppini, P. Oddo, and A. Iafrati. VISIR-I: small vessels – least-time nautical routes using wave forecasts. Geoscientific Model Development, 9(4):1597–1625, 2016.

G. Mannarini and L. Carelli. VISIR-1.b: ocean surface gravity waves and currents for energy-efficient navigation. Geoscientific Model Development, 12(8):3449–3480, 2019.

Seck-Hong, C.H.U.E., 1977. New formulas for wave forecasting. In 6th Australasian Hydraulics and FluidMechanics Conference, Adelaide, Australia (pp. 165-169).

Wilson, B.W., 1965. Numerical prediction of ocean waves in the North Atlantic for December, 1959. Deutsche Hydrografische Zeitschrift, 18(3), pp.114-130.

MAN Diesel & Turbo: Basic Principles of Ship Propulsion available at: https://spain.mandieselturbo.com/docs/librariesprovider10/sistemas-propulsivos-marinos/basic-principles-of-ship-propulsion.pdf?sfvrsn=2